

Comparison of Laser-based Person Tracking at Feet and Upper-Body Height

Konrad Schenk, Markus Eisenbach,
Alexander Kolarow, and Horst-Michael Gross *

Neuroinformatics and Cognitive Robotics
Ilmenau University of Technologies

Abstract. In this paper, a systematic comparative analysis of laser-based tracking methods, at feet and upper-body height, is performed. To this end, we created a well defined dataset, including challenging but realistic person movement trajectories, appearing in public operational environments, recorded with multiple laser range finders. In order to evaluate and compare the tracking results, we applied and adapted a performance metric, known from the Computer Vision area. The dataset in combination with this performance metric enables us to perform systematic and repeatable experiments for benchmarking laser-based person trackers.

Keywords: Laser Range Finder, Person Tracking, People Tracking, Feet Height, Upper-Body Height, MOTP, Benchmark

1 Introduction

Detecting and tracking persons with laser range finders is a common method in the field of intelligent service robotics. On a robotic platform, the laser range finder is often placed at feet height ($\approx 20\text{cm}$ above ground), to safely navigate around other objects. Additionally, this configuration is also used for person tracking. Another possible configuration is the positioning at upper-body height ($\approx 110\text{cm}$ above ground). This may produce better tracking results. Yet, this is not evaluated, since most common robotic platforms do not have laser range finders at upper-body height. Other research groups focus on people tracking with multiple laser range finders. Multiple lasers can be used for surveillance of large public areas, e.g. airports and for passenger traffic flow control. In such a scenario, a comparison of the tracking quality between feet and upper-body height was not performed. In this paper, we address this comparison.

We compare two state of the art algorithms for person tracking with multiple laser range finders at feet and upper-body height. The algorithms are evaluated in several experiments, using a representative generic dataset. A novel quality metric is used in order to compare alternative tracking algorithms for person

* This reserach was funded by the German Federal Ministry of Education and Research (BMBF) as part of the project APFeL.

tracking using laser range finders. The results can be used for selecting a suitable algorithm for a designated operational environment.

The scenario we focus on, is the surveillance of an airport. The tracking of people is achieved by cameras, but we additionally use the laser range finders to extract a global movement model and a prediction graph between all cameras. Such a graph is important, since the cameras do not overlap, and a global tracking needs additional information for correct interpolation of trajectory pieces, between different cameras.

The remainder of this paper is organized as follows: We present the state of the art for tracking persons with laser range finders at feet and upper-body height in Section 2. The most promising and real-time capable tracking algorithms are also described in this section in more detail. These trackers were then used in our experiments (Section 3). Additionally, we present the experimental setting, our test framework, and the experiments including a detailed comparison between the two setups. We complete with a conclusion and a perspective on further work.

2 Tracker

Laser range finders have been widely used for people tracking. Most applications on mobile robotic platforms use one finder at feet height [2, 11, 13, 17]. Also static installations at feet height were used in research [1]. An elaborated detection mechanism on feet height, which could be used with a generic tracking mechanism, was presented in Arras et al. [3]. Shao et al. [14] utilized a multi-person tracking mechanism using multiple stationary laser range finders at feet height in combination with a sophisticated motion model.

Only little research was conducted on upper-body height. In [6] and [9], hybrid mechanisms for tracking people at feet height and upper-body height were developed for a mobile robot. In [10], multiple static laser range finders were utilized to predict the movements of people in a public area. Glas et al. [8] also employs multiple static laser range finders at upper-body height, in order to track people and improve self localization of mobile robots.

The usage of scans at multiple heights was also investigated in [12, 15]. The evaluation of these novel methods may lead to promising results in further work.

For comparison, we have chosen the feet tracker of Shao [14], since it can be implemented with real time capabilities and proves good results. Additionally the use of a background model simplifies the detection of people. The tracking mechanism presented by Glas et al. [8] also provides a good tracking performance. We use a similar, but simpler, real-time multi person tracker for the laser range finders at upper-body height.

In order to track people in laser range data, several tasks need to be addressed. At first, an adequate preprocessing of the data is needed. Afterwards, the tracking itself can be performed. Both tasks are now shortly described.

In the preprocessing, all laser range finders are aligned in a global coordinate system. This way, the range scans from all laser finders can be transformed into

a global set of points. In the next step, we perform a histogram-based background subtraction. This enables us to extract all points referring to dynamic objects. Solely, those points are used to track the people. Afterwards, a mean shift clustering, similar to the work in [7] (which is also used in [14]), is applied, in order to segment the point clouds into clusters. Those clusters are used to detect people afterwards.

Under the assumption, that people’s movement is Markovian, both tracking methods apply multiple particle filters for estimating the current state of all people. A simple particle filter, as described in [16], is used in both tracking methods.

2.1 Feet Tracker

The used feet tracker follows the implementation of [14]. Every person is tracked by an individual particle filter. In order to initialize a filter, a person needs to be detected. This is done by spatio-temporal analysis of the clusters obtained by the mean shift algorithm. When a foot is pivoting around the other one, a certain sequence can be observed in the clustered points, which can be seen in Figure 1. At first, every foot has its own cluster of points. After the distance of the moving

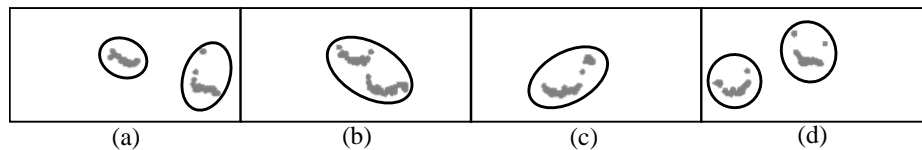


Fig. 1. Merging and splitting of the clusters belonging to the feet of a person. The person is walking from right to left, while the right foot is standing and the left one is passing by. In (a), both feet have their own cluster. In (b) and (c), both feet are close enough to cause their scan points to be merged into one cluster. In (d), the left foot reached a distance high enough from the right foot, so that the big cluster is split up into two clusters again.

foot to the standing foot falls below a certain threshold, the points of both feet are merged into one cluster. If the moving foot departs from the standing foot afterwards, the big cluster is split up into two clusters again. Therefore, a person walking one step can be detected at two specific time frames. In order to detect a splitup or a merge, it is sufficient to analyze the overlapping areas of the clusters in two adjacent time frames. After such a sequence is found, a particle filter can be initialized at this position, in order to track the newly detected person.

The state \mathbf{z}_t of one persons movement consists of eight parameters: (x_t^l, y_t^l) and (x_t^r, y_t^r) are the positions of the left and right feet, s_t is the walking stride, T_t the walking period, α_t the walking direction and γ_t the walking phase.

The walking model implements a periodic function and is described in Equation 1 and 2, where δ is the duration between the last and the current time step.

Further details and the derivation can be found in [14].

$$\begin{aligned}
& \text{if } (\text{mod}(\gamma_t, 2\pi) > \pi) \\
& \quad m_l = s_t |\cos(\gamma_t) - \cos(\gamma_{t-1})| \\
& \quad m_r = 0 \\
& \text{else} \\
& \quad m_l = 0 \\
& \quad m_r = s_t |\cos(\gamma_t) - \cos(\gamma_{t-1})| \\
& \text{end}
\end{aligned} \tag{1}$$

$$\begin{pmatrix} x_t^l \\ y_t^l \\ x_t^r \\ y_t^r \\ s_t \\ T_t \\ \gamma_t \\ \alpha_t \end{pmatrix} = \begin{pmatrix} x_{t-1}^l \\ y_{t-1}^l \\ x_{t-1}^r \\ y_{t-1}^r \\ s_{t-1} \\ T_{t-1} \\ \gamma_{t-1} \\ \alpha_{t-1} \end{pmatrix} + \begin{pmatrix} \cos(\alpha_{t-1}) \cdot m_l \\ \sin(\alpha_{t-1}) \cdot m_l \\ \cos(\alpha_{t-1}) \cdot m_r \\ \sin(\alpha_{t-1}) \cdot m_r \\ 0 \\ 0 \\ 2\pi \frac{\delta}{T_{t-1}} \\ 0 \end{pmatrix} \tag{2}$$

The observation model takes the scan points directly into account. If $Z = \{x^{(j)}, y^{(j)} | j = 1, \dots, N\}$ are the observed foreground points, the weight of a sample can be updated with Equation 3–7. For further details, please refer to [14].

$$o_l = \max \left(\sum_{j=1}^N \exp \left(-\frac{(x_t^l - x^{(j)})^2 + (y_t^l - y^{(j)})^2}{2\delta^2} \right), P_0 \right) \tag{3}$$

$$o_r = \max \left(\sum_{j=1}^N \exp \left(-\frac{(x_t^r - x^{(j)})^2 + (y_t^r - y^{(j)})^2}{2\delta^2} \right), P_0 \right) \tag{4}$$

$$s_d = (x_t^r - x_t^l) \cdot \cos(\alpha_t) + (y_t^r - y_t^l) \cdot \sin(\alpha_t) \tag{5}$$

$$o_b = \exp \left(-\frac{(s_d + s_t \cdot \cos(\gamma_t))^2}{2h^2} \right) \tag{6}$$

$$w_t^{(i)} = o_l \cdot o_r \cdot o_b \tag{7}$$

When two persons are walking in a close proximity, particle filters can switch to people already being tracked. Therefore, a repelling term between the filters is included to avoid hijacking. This ensures, that one person is only tracked by a single particle filter.

2.2 Upper-Body Tracker

For the upper-body tracker we utilize a more common approach, similar to [8]. Every person is tracked by an individual particle filter. The detection of a person is done by evaluating the size of a scan point cluster, using its eigenvalues.

A threshold for the biggest eigenvalue describes the minimal human body size. The upper boundary of the cluster sizes is given by the mean shift algorithm and does not need to be evaluated. In order to track the corresponding person, a particle filter is initialized at the cluster position. A more comprehensive detection method could also be applied, but due to the background subtraction, this simple approach is sufficient.

The state \mathbf{z}_t of a person consists of four parameters. (x_t, y_t) is the position of the person, α_t the movement direction and v_t the velocity along this direction. The motion model implements a simple linear movement, as shown in Equation 8, where δ is the duration between the last and the current time step.

$$\mathbf{z}_t = \begin{pmatrix} x_t \\ y_t \\ \vartheta_t \\ v_t \end{pmatrix} = \mathbf{z}_{t-1} + \begin{pmatrix} \cos(\vartheta_{t-1}) \\ \sin(\vartheta_{t-1}) \\ 0 \\ 0 \end{pmatrix} \cdot \delta \cdot v_{t-1} \quad (8)$$

The observation model for the upper-body tracker also takes the scan points directly into account. If $Z = \{x^{(j)}, y^{(j)} | j = 1, \dots, N\}$ are the observed foreground points, the weight of a sample can be updated with Equation 9.

$$w_t^{(i)} = \sum_{j=1}^N \exp \left(\frac{- \left((x_t^{(i)} - x^{(j)})^2 + (y_t^{(i)} - y^{(j)})^2 \right)}{\zeta^2} \right) \quad (9)$$

To prevent a particle filter to focus on a person already tracked by another one, only points in its proximity are used in the weight update. The proximity is evaluated by Voronoi clustering (see [18]).

Both tracking methods proved to have real-time capabilities and were used to obtain the results described in the next section.

3 Experiments

In the previous section, we introduced the selected algorithms for tracking persons with laser range finders at feet and upper-body height. Here, we compare them in several categories, including different walking speed, linear and non-linear trajectories, speed and direction changes, multiple persons, and accessories carried by people.

3.1 Experimental Setup

The experiments were conducted in a room, measuring $5.5 \times 11\text{m}$. The test persons followed specified lines on the floor. Four laser range finders were used. Two were installed at feet height (20cm) and two at upper-body height (110cm), standing at the same position. They were placed 2m left and right to the center of the trajectory. Another alternative configuration with all laser range finders

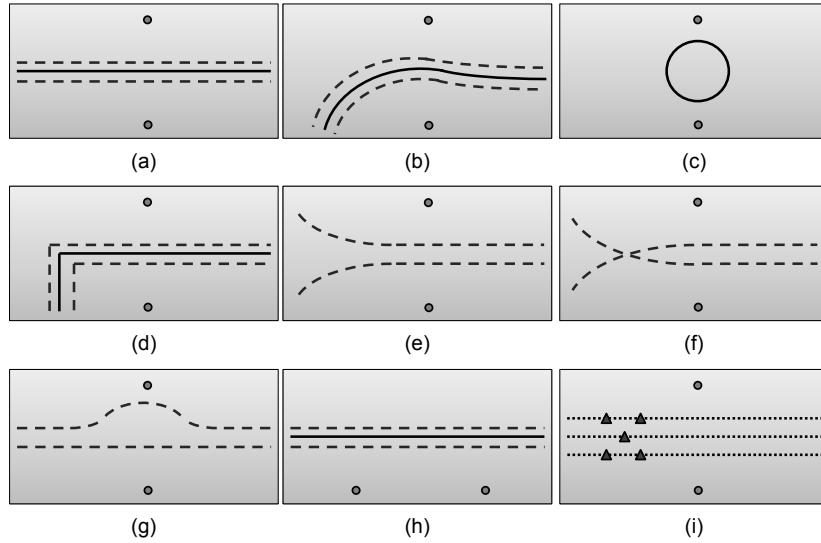


Fig. 2. Specified test trajectories. (a,h,i) Straight line, (b) Curve, (c) Circle, (d) Corner, (e) Join, (f) Cross, (g) Evading – for one (continuous line), two (dashed lines), three (dotted lines) and five persons (triangles on dotted lines). The positions of the laser range finders are marked as filled circles: (a-g,i) normal setup with laser range finders on opposite sides, (h) alternative setup with laser range finders on the same side.

installed on one side of the room was evaluated. But since no different results were obtained, we do not describe this subaspect in more detail. Seven kinds of trajectories were included in the experiments: Straight line, curve, circle, corner, join, cross and evading. Figure 2 shows all specified trajectories. The used laser range finder is LMS151 from SICK. It scans 270° with a 0.5° resolution at 50Hz. Small people or children are not harmed by the laser at upper-body height, since it is eye safe.

In the following, we describe the experiments in detail. Each experiment was based on typical situations, observed at airports. The result of one test run is shown in Figure 3.

In experiment 1 "Speed", the person walked with three different speeds (slow, normal, fast) on a straight line (Figure 2a). For each speed, three different persons were recorded three times, resulting in nine trajectories (for all following experiments also nine trajectories were extracted).

Experiment 2 "Non-linear trajectories" examined the tracker for a single person walking on curves. Experiments included a curve (Figure 2b), a circle (Figure 2c) and evading (Figure 2g). This tested the ability of the algorithms to track non-linear movements.

In experiment 3 "Change of direction and speed", sudden changes of the walking direction or speed were evaluated. The direction change was emulated

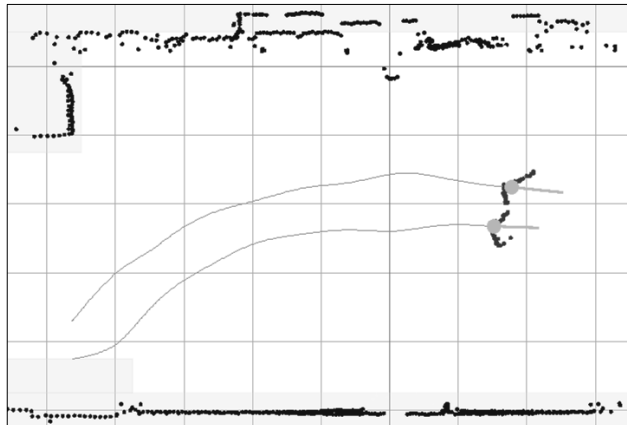


Fig. 3. Single exemplary tracking result of trajectory (b).

by a single person walking on trajectory (d) of Figure 2. The speed changed when the person stopped at the middle of the trajectory (a), waited some time and moved on. In a third test, the persons were additionally asked to stop and turn around in order to look behind. This experiment addressed the ability to track persons with non-linear movements.

Experiment 4 "Multiple persons" examined the tracking precision with an increasing number of people. In the case of multiple persons in the scene, occlusions appeared more often. The tracker had to cope with only partly visible and fully occluded persons. Trajectories (a,b,d) from Figure 2 were used for two and three persons and trajectory (i) for five persons.

In experiment 5 "ID switch", the ability to differentiate trajectories of persons, walking close to each other, was evaluated. Two cases were considered: In the first case, the trajectories of the two persons drew near but did not cross (Figure 2e). In the second case the trajectories intersected (Figure 2f). The tracker needed to follow the two persons without switching the IDs.

Experiment 6 "Accessories" tested the influence of accessories to the tracking result. The following situations were considered: persons carrying and pulling suitcases, pushing a baggage cart, carrying large items in front of the body, using a cane and wearing a shoulder bag or a long skirt. For this experiment, we used trajectory (a) from Figure 2.

3.2 Precision Measure

In order to evaluate the tracking results, we adapt the multi object tracking precision (MOTP), a widely used measure in computer vision. The original approach uses the overlap between the bounding boxes of the tracker's hypothesis and the ground truth bounding boxes of the objects of interest, e.g. persons, in every frame. Details can be found in [4, 5].

In the following, we present our adapted version for laser-based tracking. In contradiction to the bounding box in computer vision, the tracked object is represented by a point, when using laser range finders. Therefore, we can not utilize the overlap with the ground truth. Instead, we use the distance. The matching value (m) should be 1, if the distance is smaller than a threshold (similar to a minimum overlap), and between 0 and 1 otherwise. We defined the following matching term:

$$m = \min\left(1, \frac{h}{d^3}\right), \quad (10)$$

where d is the distance to the ground-truth in meters, and h is a threshold. We use $h = 0.008$ which values a hypothesis correct, if $d \leq 20$ cm.

The remaining calculations are inherited from the original MOTP: First, every trajectory of the tracker (T) has to be matched to the best suitable ground truth trajectory (G). Every trajectory T can only be matched to one trajectory G and vice versa. If the amount of trajectories T is smaller than the amount of trajectories G, virtual trajectories T are added with a matching term of $m = 0$. Unmatched trajectories T also get a matching term of $m = 0$. With this combinatoric problem solved, the MOTP can be calculated as

$$MOTP = \frac{\sum_{i=1}^F \sum_{j=1}^{N_i^G} m_{ij}}{\sum_{i=1}^F \max(N_i^T, N_i^G)}, \quad (11)$$

where F is the number of frames, m_{ij} is the matching value between ground truth trajectory j and its belonging trajectory T in frame i (Equation 10). N_i^T and N_i^G are the number of trajectories T and trajectories G in frame i .

In Figure 4, we show exemplary trajectories and their MOTP. The measure with the recommended threshold gives a very intuitive interpretation of the result. If the tracking result is very similar to the ground truth, the MOTP is

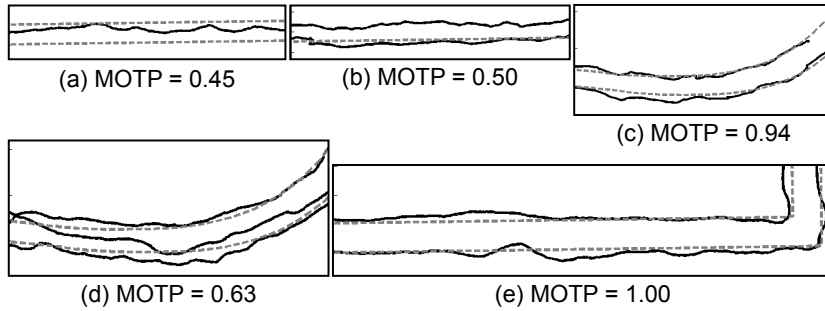


Fig. 4. Spatial plot of example trajectories in topview. Continuous lines represent the calculated trajectories and dashed lines represent the ground truth. Corresponding MOTP are shown below the plots.

1.0 (Figure 4e). One particle filter tracking two persons results in a MOTP near 0.5 (Figure 4a). Similar, two particle filters tracking a single person, also results in a MOTP near 0.5 (Figure 4b), and three filters tracking two persons result in a MOTP near $\frac{2}{3}$ (Figure 4d). The MOTP decreases whenever gaps in the trajectories are present or the trajectory is too far away from the ground truth (Figure 4c). When a particle filter, belonging to person A, switches to another person B, it has a high distance to its original ground truth. This ID-switch is penalized, since the high distance of person B to the ground truth of A results in a low MOTP.

3.3 Results Feet Tracker

Table 1–3, 5 and 6 show, that despite the difficult setups, the feet tracker has achieved good results. In contrast, high initial speeds of people can cause the feet tracker to fail, as shown in Table 1. While running, the movement of people’s feet differs, compared to normal walking. The motion model of the feet tracker is not designed to track those running movements and therefore fails tracking.

Movements of one or two persons pose no problem. Three or five people walking in close proximity to each other, are resulting in erroneous tracking. This can be ascribed to the initialization of the particle filters. Particle filters, for people entering the scene, are not initialized immediately. As described in Section 2.1, detections are only triggered at specific time frames. Therefore, particle filters for multiple persons, entering the scene at the same time, are not initialized at the same moment. Persons not being tracked by a particle filter, disturb nearby particle filters. Occlusions can also prevent the tracking mechanism from detecting a person for a longer period of time. This can cause identity switches and tracking errors as shown in Table 4.

Moving objects, other than the feet, also disturb the tracking mechanism. The suitcase and the baggage cart, mentioned in Table 6, cause scan points in the proximity of the tracked person. Therefore, the corresponding particle filter is often hijacked, or fails to estimate the movement parameters. This leads to bad tracking results.

3.4 Results Upper-Body Tracker

The upper-body tracker achieves very good results in nearly every experiment. But multiple people walking in close proximity to each other can cause the tracker to fail. This is shown in Table 4. The failures are caused by occlusions and identity switches: If a person is occluded for some time, its particle filter is often hijacked by a nearby person. As shown in Table 6, a baggage cart can disturb the tracking mechanism, too. The cart is detected by the laser range finders at upper-body height and causes a second particle filter to be initialized. Therefore, the baggage cart, and the person pushing it, are tracked, which results in a bad assessment of the tracker in such a case.

Table 1. Experiment 1
"Speed"

Scene	FT	UBT
slow	1.0	1.0
normal	0.84	1.0
fast	0.50	0.88
Avg.	0.78	0.96

Table 2. Experiment 2
"Non-linear trajectories"

Scene	FT	UBT
curve	0.83	1.0
circle	0.78	0.99
evading	0.97	0.95
Avg.	0.86	0.98

Table 3. Experiment 3
"Change of direction and speed"

Scene	FT	UBT
corner	0.83	0.89
stop	0.81	0.91
turn	0.84	0.90
Avg.	0.83	0.90

Table 4. Experiment 4
"Multiple persons"

Scene	FT	UBT
1 pers.	0.84	1.0
2 pers.	0.85	0.90
3 pers.	0.57	0.91
5 pers.	0.53	0.66
Avg.	0.70	0.87

Table 5. Experiment 5
"ID switch"

Scene	FT	UBT
join	0.81	0.87
cross	0.81	0.97
Avg.	0.81	0.92

Table 6. Experiment 6
"Accessories"

Scene	FT	UBT
carry case	0.78	0.96
pull case	0.32	1.0
carrying	0.86	1.0
bag	0.86	1.0
skirt	0.86	0.95
cane	0.88	1.0
cart	0.45	0.69
Avg.	0.72	0.94

The results are obtained by using the MOTP metric (see Section 3.2). FT is referring to the results of the feet tracker, while UBT refers to the upper-body tracker.

3.5 Comparison and Discussion

Both tracking methods performed well, but in nearly every experiment, the upper-body tracker achieved better results. It needs to be mentioned, that the experiments focused on difficult situations, which are not occurring in real applications frequently. Therefore, the results presented in [14] are plausible, despite of the results their tracking method achieved in our experiments.

The main difference between both tracking methods is the motion model. The feet tracker implements a motion model, dedicated for walking movements of human feet, with eight parameters. The upper-body tracker uses a simpler linear motion model with four parameters. Therefore, it is more difficult for the feet tracker to estimate the correct motion parameters, since a larger parameter space has to be covered. Hence, the feet model is more likely to fail in case of disturbances, like occlusions in combination with other nearby objects, or changes in movement. This seems to be the main cause for the slightly better performance of the upper-body tracker.

Different movement speeds only affect the feet tracker. As shown in Table 1, the specialized motion model of the feet tracker is only able to describe regular walking movements, which are not present in the recordings of fast speed. A running movement differs from the regular and causes failures in tracking.

As Table 2 and 3 show, non-linearities and changes in movement do not pose a problem for both tracking methods. The use of particle filters implements a certain random element compensating for these variations in movement.

Since a certain sequence of observations is required to trigger a detection within the feet tracker, particle filters can only be initialized at specific time frames. The upper-body tracker can detect a person at every time step, as long as no occlusions are present. Therefore, every person entering the scene is tracked immediately by the upper-body tracker and does not influence other particle filters. Thus, the feet tracker mainly fails in tracking multiple people, due to unfavorable conditions during initialization. The upper-body tracker primarily fails in tracking multiple people, due to identity switches, caused by occlusions. This leads to the results, shown in Table 4.

As Table 5 proves, both tracking mechanisms do not switch their targets in experiment 5. Nevertheless, identity switches may happen in more complex situations, as described in the previous paragraph.

Both tracking methods show problems with objects near the tracked persons (see Table 6). The baggage cart in experiment 6 causes scan points on both heights. It hijacks the particle filter at feet height, or causes false detections on the upper-body height. However, objects in close proximity to the person at upper-body height did not cause any problems, since their scan points were joined into the cluster of the person. Most accessories, like suitcases, are only visible at feet height. Therefore, they do not influence the upper-body tracker.

The upper-body tracker benefits from a simpler movement model and less disturbances, caused by non human objects. The feet tracker profits from less occlusions, due to the geometry of people. Another advantage of the feet tracker is the simpler installation, since no tripod or stand is required.

4 Conclusion

For the first time, a qualitative and quantitative comparison of two laser-based tracking methods was performed and their flaws and advantages were discussed in detail. In order to ensure a fair comparison, we recorded a huge dataset of laser range scans at feet and upper-body height. With a total of 55 minutes of scandata, containing 696 single recordings with more than one thousand individual person movement trajectories, we obtained more than 650 000 single laser range scans. The MOTP metric was adapted, in order to evaluate laser-based tracking results. The dataset in combination with the new metric provides a benchmarking framework, which can be used for choosing a suitable tracking mechanism for a designated operational environment.

In our scenario, the surveillance of an airport, the upper-body tracker is in advantage, since accessories like suitcases and skirts do not influence the tracking. However, a combination of scans at upper-body and feet height, like in [6, 9], might improve the detection and tracking of people.

In our future work, we intend to offer an extended version of the dataset in combination with an evaluation framework, utilizing the introduced metric.

Thus, we enable other research groups to benchmark their tracking methods for comparison. The extended dataset will include more setups, in order to widen the scope, beyond regular movements and airport scenarios. Furthermore, other tracking methods and the influence of their parameters will be evaluated.

References

1. Almeida, A., Almeida, J., Araujo, R.: Real-time tracking of moving objects using particle filters. In: ISIE. pp. 1327–1332 (2005)
2. Arras, K., Grzonka, S., Luber, M., Burgard, W.: Efficient people tracking in laser range data using a multi-hypothesis leg-tracker with adaptive occlusion probabilities. In: ICRA. pp. 1710–1715 (2008)
3. Arras, K., Mozos, O., Burgard, W.: Using boosted features for the detection of people in 2d range data. In: ICRA. pp. 3402–3407 (2007)
4. Bernardin, K., Elbs, A., Stiefelwagen, R.: Multiple object tracking performance metrics and evaluation in a smart room environment. In: 6th IEEE International Workshop on Visual Surveillance (2006)
5. Bernardin, K., Stiefelwagen, R.: Evaluating multiple object tracking performance: The clear mot metrics. EURASIP IVP (2008)
6. Carballo, A., Ohya, A., Yuta, S.: Fusion of double layered multiple laser range finders for people detection from a mobile robot. In: MFI. pp. 677–683 (2008)
7. Comaniciu, D., Meer, P.: Distribution free decomposition of multivariate data. PAA 2(1), 22–30 (1999)
8. Glas, D.F., et al.: Simultaneous people tracking and localization for social robots using external laser range finders. In: IROS. pp. 846–853 (2009)
9. Hashimoto, M., Konda, T., Bai, Z., Takahashi, K.: Laser-based tracking of randomly moving people in crowded environments. In: ICAL. pp. 31–36 (2010)
10. Kanda, T., et al.: Who will be the customer?: A social robot that anticipates people’s behavior from their trajectories. In: UbiComp. pp. 380–389 (2008)
11. Lee, J.H., Tsubouchi, T., Yamamoto, K., Egawa, S.: People tracking using a robot in motion with laser range finder. In: IROS. pp. 2936–2942 (2006)
12. Mozos, O., Kurazume, R., Hasegawa, T.: Multi-part people detection using 2d range data. IJSR 2, 31–40 (2010)
13. Schulz, D., et al.: People tracking with mobile robots using sample-based joint probabilistic data association filters. IJRR 22(2), 99–116 (2003)
14. Shao, X., et al.: Tracking a variable number of pedestrians in crowded scenes by using laser range scanners. In: SMC. pp. 1545–1551 (2008)
15. Spinello, L., Luber, M., Arras, K.O.: Tracking people in 3d using a bottom-up top-down people detector. In: ICRA. pp. 1304–1310 (2011)
16. Thrun, S., Burgard, W., Fox, D.: Probabilistic Robotics. MIT Press (2005)
17. Topp, E.A., Christensen, H.I.: Tracking for following and passing persons. In: IROS. pp. 70–76 (2005)
18. Voronoi, G.: Nouvelles applications des paramètres continus à la théorie des formes quadratiques. Deuxième mémoire. Recherches sur les paralléloèdres primitifs. Journal für die reine und angewandte Mathematik 1908(134), 198–287 (1908)